ELSEVIER

Journal of Power Sources 103 (2001) 86–92

JOURNAL OF POWER SOURCES

www.elsevier.com/locate/jpowsour

# Improvement of the rate capability of $LiMn_2O_4$ by surface coating with $LiCoO_2$

Sung-Chul Park, You-Min Kim, Yong-Mook Kang, Ki-Tae Kim, Paul S. Lee, Jai-Young Lee*

*Department of Materials Science and Engineering, Korea Advanced Institute of Science and Technology, 373-1 Kusong-Dong, Yusong-Gu, Taejon 305-701, South Korea*

Received 6 October 2000; received in revised form 20 December 2000; accepted 5 June 2001

**Abstract**

In order to use $LiMn_2O_4$ as a cathode material of lithium-secondary battery for an electric vehicle (EV), its rate capability should be improved. To enhance the rate capability of $LiMn_2O_4$ in this work, the surface of $LiMn_2O_4$ particle was coated with $LiCoO_2$ by a sol–gel method. Because $LiCoO_2$ has a higher electric conductivity than $LiMn_2O_4$, it is possible to improve the rate capability of $LiMn_2O_4$. After the surface coating, $LiCoO_2$-coated $LiMn_2O_4$ showed a higher discharge capacity of 120 mAh/g than as-received $LiMn_2O_4$ (115 mAh/g) because $LiCoO_2$ has a higher capacity than $LiMn_2O_4$. The rate capability of the coated $LiMn_2O_4$ improved significantly. While as-received $LiMn_2O_4$ maintained only 50% of its maximum capacity at a 20*C* rate (2400 mA/g), the $LiCoO_2$-coated $LiMn_2O_4$ maintained more than 80% of maximum capacity. $LiCoO_2$-coated $LiMn_2O_4$ with 3 wt.% conducting agent (acetylene black) showed the higher rate capability than as-received $LiMn_2O_4$ with 20 wt.% conducting agent. From electrochemical impedance spectroscopy (EIS) result that the first and second semicircles of coated $LiMn_2O_4$ were reduced, the improvement of rate capability is attributed to a decrease of passivation film that acts as an electronic insulating layer and a reduced inter-particle contact resistance. Accordingly, It is proposed that the surface coating of $LiMn_2O_4$ with $LiCoO_2$ improve the rate capability as well as the specific and volumetric energy density due to the decrease of conducting agent. 

*Keywords:* Lithium-secondary battery; Surface coating; Sol–Gel method; $LiMn_2O_4$; $LiCoO_2$; Rate capability

## 1. Introduction

Since the first commercialization by Sony Energytech in the early 1990s, the lithium-ion rechargeable battery (LIB) has become a major product to dominate the market for small rechargeable batteries [1,2]. Furthermore, Li-ion batteries are expected to be used as a large-scale energy storage device for electric vehicles (EV) as well as for electric power load leveling system [3–5].

Though commercialized Li-ion batteries are currently using various types of cathode material such as $LiCoO_2$, $LiNiO_2$, $LiMn_2O_4$, and a substituted transition metal oxides ($LiNi_{1-x}Co_xO_2$), $LiCoO_2$ in these cathode materials is most widely used because it has an excellent cycle life and it is relatively more stable against thermal decomposition in charged state than nickel based materials [6,7]. However, as cobalt is an expensive and relatively rare transition metal, attention has been paid to $LiMn_2O_4$ pursuing the advantages of low cost and environmental affinity. Especially, the good thermal behavior of $LiMn_2O_4$ is a positive factor for a large-scale battery to be used for EV because it is not necessary to equip the expensive safety devices [8].

However, the pure lithium manganese oxide has a poor cycle stability and an insufficient rate capability. It is reported that the capacity fading mechanism of the pure lithium manganese oxide at room temperature is related to the Jahn–Teller distortion caused by the presence of $Mn^{3+}$ Jahn–Teller ions [9]. The Jahn–Teller distortion could be reduced with the cation substitution for Mn in the 16d sites. For instance, $LiMn_{2-y}Co_yO_4$ ($y = 0.1$) or $LiMn_{2-y}Li_yO_4$ ($y = 0.05$) were reported to have the excellent cycle stability at room temperature because of the decrease of $Mn^{3+}$-ions [10–12].

In spite of the success in improving cycle stability, little has been reported on the enhanced rate capability of $LiMn_2O_4$. In particular, it is necessary to improve the rate capability of $LiMn_2O_4$-spinel in order to use it as a cathode material of LIB for EV. The reason for poor rate capability of

* Corresponding author. Tel.: +82-42-869-3313; fax: +82-42-861-0950.
*E-mail address*: jailee@mail.kaist.ac.kr (J.-Y. Lee).

0378-7753/01/$ – see front matter 
PII: S0378-7753(01)00832-1

$LiMn_2O_4$ is not clear but it may be attributed to its low electrical conductivity ($10^{-6}$ S/cm) [13]. The low electric conductivity of $LiMn_2O_4$ can limit the current flow between particles, which may decrease its rate capability. Therefore, $LiMn_2O_4$ needs more conducting agent to obtain the sufficient rate capability property in comparison with $LiCoO_2$. Because large amount of conducting agent decreases the energy density of battery, the amount of conducting agent should be minimized. It indicates that the increase in electric conductivity of $LiMn_2O_4$ can improve its rate capability without decreasing energy density.

In the present study, the surface of $LiMn_2O_4$ was encapsulated with small $LiCoO_2$ particles, which has a higher electric conductivity ($10^{-2}$ S/cm) than $LiMn_2O_4$, in order to reduce the inter-particle resistance and improve its rate capability [13]. The effects of its surface coating with $LiCoO_2$ on rate capability of $LiMn_2O_4$ were also investigated.

## 2. Experimental

### 2.1. Preparation of $LiCoO_2$-coating solution and coating of $LiMn_2O_4$ with $LiCoO_2$

The coating solution to encapsulate the surface of $LiMn_2O_4$ was prepared by the sol–gel process. Stoichiometric amounts of lithium acetate ($Li(CH_3COO)\cdot 2H_2O$, 98% Aldrich) and cobalt acetate ($Co(CH_3COO)_2\cdot 4H_2O$, 99% Aldrich) with a cationic ratio of Li:Co = 1:1 were dissolved in distilled water and stirred at 50–60°C. An aqueous glycolic acid water solution ($HOCH_2CO_2H$, 70% Aldrich) as a chelating agent was then added to this mixture solution to produce a gel-type solution. The molar ratio of glycolic acid to total metal ions was fixed at 1.5. Then ammonium hydroxide was added slowly to this solution with constant stirring until the pH value of 6.5–7.0 was achieved. This last solution was thoroughly mixed and reacted in refluxing system for 6 h at 80–90°C. The resultant solution was evaporated at about 80°C until its concentration reached about 1 mol/l. The commercial $LiMn_2O_4$ powder was then added to this resultant coating solution and the mixture was stirred. Afterwards, $LiMn_2O_4$ immersed in this coating solution was screened with a centrifuge. The screened powder was dried in a vacuum oven and calcined for 6 h at 800°C.

### 2.2. Measurement of structural and electrochemical properties

For the structural analysis, the $LiCoO_2$-coated $LiMn_2O_4$ samples were characterized with X-ray diffraction (XRD) with Cu Kα radiation (Rigaku D/MAX-IIIC) and transmission electron microscopy (TEM, Hitachi Company). The morphology of a coated-sample was observed with a scanning electronic microscope (SEM). The amount of a coating material in the coated-samples was determined by inductively coupled plasma (ICP).

For the fabrication of the cathode, the spinel powder was mixed with acetylene black as a conducting agent and polyvinylidene fluoride (PVDF) as a binder in a various mass ratio of 94–75:1–20:5. The $LiMn_2O_4$-spinel powder and acetylene black powder were first added to a solution of PVDF in *N*-methyl-2-pyrrolidinone (NMP) to make the slurry with appropriate viscosity. Then the slurry was spread on to an Al foil current-collector and dried at 140°C for 2 h in vacuum ($10^{-3}$ Torr). After drying the electrodes, they were compressed to a desired thickness (50 μm) and cut into to be a same size. Coin cells were assembled in an argon filled glove-box, where the counter electrode was a Li metal and the electrolyte was a 1 M $LiPF_6$ dissolved in a 50/50 vol.% mixture of ethylene carbonate (EC) and diethyl carbonate (DEC).

For the electrochemical analysis, these cells were cycled between 3.0 and 4.3 V with the current rate range of 12–2400 mA/g (0.1–20*C* rate). In addition, potentiostatic charge–discharge tests were carried out with cyclic voltammetry (CV) at both scan rates of 0.01 and 0.05 mV/s. For the electrochemical impedance measurements, a Solatron 1255 frequency response analyzer was used in conjunction with the Solatron 1286 electrochemical interface. After the electrode reached its equilibrium potential (4.1 V), the impedance measurements were carried out by applying an ac voltage of 5 mV over the frequency range from 1 mHz to 100 kHz.

## 3. Results and discussion

### 3.1. Optimization of annealing condition for $LiCoO_2$-coated $LiMn_2O_4$

Sun et al. reported that a very small powder was synthesized by sol–gel method from aqueous solution of metal acetates containing glycolic acid as a chelating agent [14,15]. In the current work, sol–gel method was used to coat the surface of $LiMn_2O_4$ with fine $LiCoO_2$ particulates. The gel precursor of $LiCoO_2$ as a coating solution surrounded the surface of $LiMn_2O_4$ before it was evaporated completely and became a powder. Afterwards, annealing was performed to crystallize its gel precursor which was spread on the surface. In order to determine the optimized annealing temperature of $LiCoO_2$-coated $LiMn_2O_4$, $LiCoO_2$ powder was synthesized from its gel precursor at various temperatures, and its structural and electrochemical properties were investigated. Fig. 1 shows XRD patterns of $LiCoO_2$ samples with various synthesis temperatures (700–850°C). All samples mainly have a α-$NaFeO_2$-type layered structure. The change of discharge capacity with synthesis temperature is shown in Fig. 2. As the synthetic temperature increased, the discharge capacity also increased because of increasing crystallinity. However, the capacity of $LiCoO_2$ synthesized at 850°C, get decreased. Therefore, the annealing temperature of $LiCoO_2$-coated $LiMn_2O_4$ powder was determined to be 800°C.

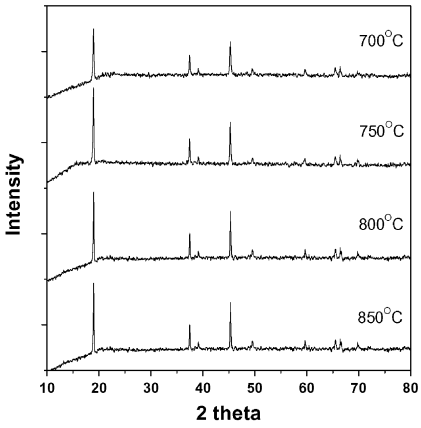


Fig. 1. XRD patterns of $LiCoO_2$ powder prepared by sol–gel method and synthesized at various temperature (700–850°C).

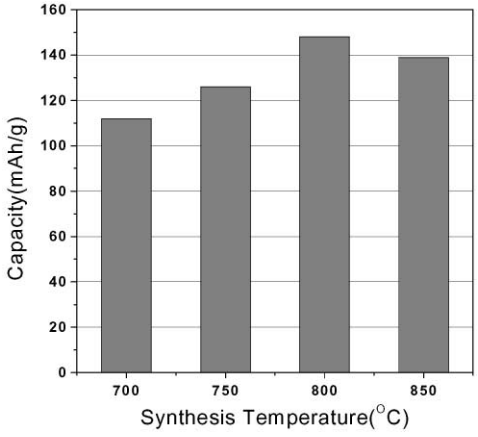


Fig. 2. Capacity change of $LiCoO_2$ powder synthesized at various temperature (700–850°C).

### 3.2. Surface morphology of as-received $LiMn_2O_4$ and $LiCoO_2$-coated $LiMn_2O_4$

Fig. 3 shows the SEM micrograph of $LiCoO_2$ powder synthesized from its gel precursor at 800°C. The particle size was very small and the size distribution was very homogeneous. So, it is expected that this $LiCoO_2$ powder can encapsulate the surface of $LiMn_2O_4$ effectively. SEM images in Fig. 4 show the surface morphology of as-received $LiMn_2O_4$ and that of $LiCoO_2$-coated $LiMn_2O_4$. The surface morphology of as-received $LiMn_2O_4$ was round and smooth as shown in Fig. 4(a). With the surface coating of $LiMn_2O_4$ with $LiCoO_2$, the surface was covered with small particles as shown in Fig. 4(b). From Figs. 3, 4(a) and (b), it can be speculated that the surface of $LiMn_2O_4$ is covered with small particles of $LiCoO_2$ powder. In order to analyze the phase of particles that exist on the surface of coated $LiMn_2O_4$, TEM analysis was performed. Fig. 5 shows the TEM image of coated $LiMn_2O_4$ and the selected-area diffraction (SAD) patterns of its outer part and inner part, respectively. From the SAD patterns of inner part (Fig. 5(b)) and outer part (Fig. 5(c)), it is found that the inner part is as-received $LiMn_2O_4$ with the spinel structure (the lattice parameter of *a*-axis: 8.237 Å) and the outer part is $LiCoO_2$ with hexagonal structure(the lattice parameter of *a*-axis: 2.819 Å), which indicates that $LiCoO_2$ phase is formed on the surface of coated $LiMn_2O_4$ by the chemical process [16,17]. However, the possibility of partial formation of Co-doped $LiMn_2O_4$ on the $LiMn_2O_4$ powder cannot be excluded owing to the

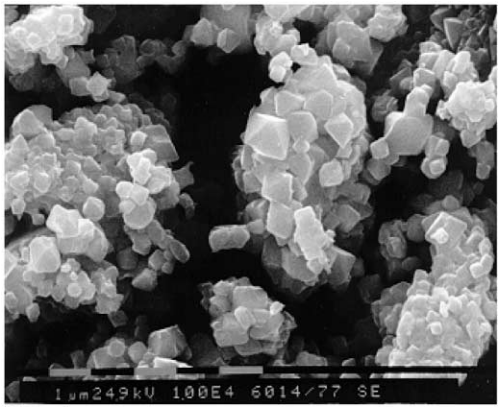


Fig. 3. SEM photograph of $LiCoO_2$ powder prepared by sol–gel method.

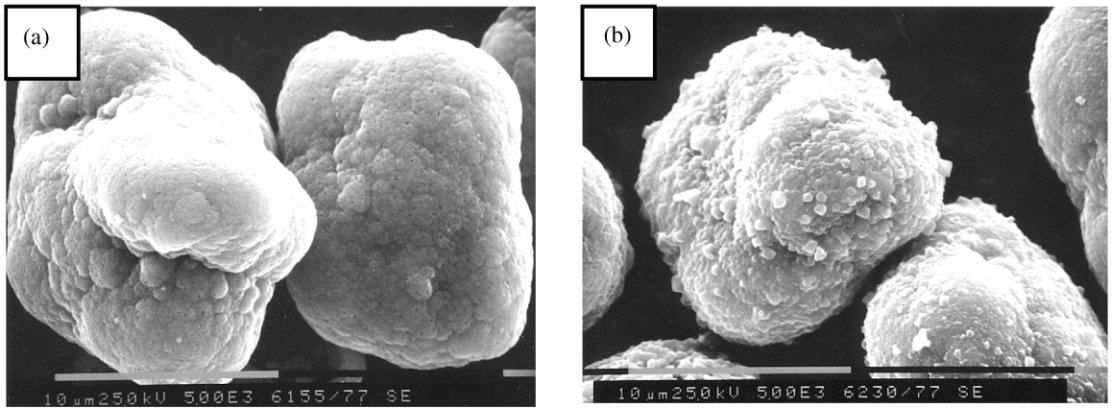


Fig. 4. SEM photographs of (a) as-received $LiMn_2O_4$ and (b) $LiCoO_2$-coated $LiMn_2O_4$ powders.

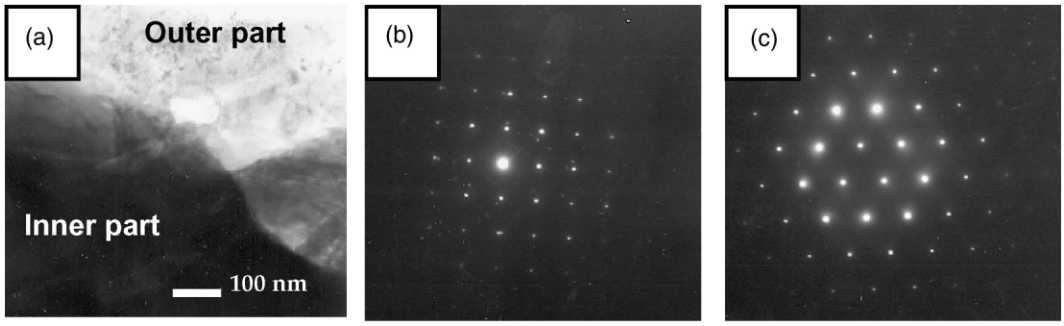


Fig. 5. (a) TEM bright-field image of coated $LiMn_2O_4$ and SAD patterns of (b) inner part ([0 0 1] projection) and (c) outer part ([0 0 0 1] projection) in coated $LiMn_2O_4$.

reaction between $LiCoO_2$ and $LiMn_2O_4$. For the analysis of cobalt content that resided on the surface of $LiMn_2O_4$, ICP analysis was performed. From the ICP analysis (Table 1), it is found that 2.2 mol% of cobalt remains on the surface of $LiMn_2O_4$.

### *3.3. Electrochemical properties of as-received $LiMn_2O_4$ and $LiCoO_2$-coated $LiMn_2O_4$*

Charge–discharge curves of as-received $LiMn_2O_4$ and $LiCoO_2$-coated $LiMn_2O_4$ are shown in Fig. 6. While the discharge capacity of as-received $LiMn_2O_4$ was 115 mAh/g, that of $LiCoO_2$-coated $LiMn_2O_4$ was 120 mAh/g. The slight increase of discharge capacity is due to a higher discharge capacity of $LiCoO_2$ than that of $LiMn_2O_4$. As well, both electrodes show two same plateaus distinctly, which means that $LiCoO_2$-coating does not change the intrinsic properties of $LiMn_2O_4$ such as crystal structure and charge–discharge behavior. In order to investigate the electrochemical behavior of as-received $LiMn_2O_4$ and $LiCoO_2$-coated $LiMn_2O_4$, the CV curve of $LiCoO_2$-coated $LiMn_2O_4$ is compared with those of as-received $LiMn_2O_4$ and $LiCoO_2$ in Fig. 7. The CV curves are taken at a scan rate of 0.05 mV/s. In comparison of Fig. 7(a) with (b), it is found that the CV curve of $LiCoO_2$-coated $LiMn_2O_4$ do not include the main current peak shown in the CV curve of $LiCoO_2$. The reason is that the concentration of $LiCoO_2$ on the surface of $LiMn_2O_4$ is very low. Both curves in Fig. 7(b), however, show a similar CV behavior with two current peaks although the current peaks of as-received $LiMn_2O_4$ are shifted to the right during charging and to the left during discharging from the peak positions of $LiCoO_2$-coated $LiMn_2O_4$. Fig. 7(c) shows the CV curves of as-received $LiMn_2O_4$ and $LiCoO_2$-coated $LiMn_2O_4$ at a slower scan rate of 0.01 mV/s to prove that the shift of current peak positions is related to the kinetic property. Both curves have almost the same shape and current peak positions. With Fig. 7, it is concluded that the surface coating with $LiCoO_2$ has little of an effect on the charge–discharge behavior of $LiCoO_2$-coated $LiMn_2O_4$ while its rate capability improves. In Fig. 8, the rate capability of as-received $LiMn_2O_4$ is compared with that of $LiCoO_2$-coated $LiMn_2O_4$. In the case of as-received $LiMn_2O_4$, the discharge capacity decreased with the increase of charge–discharge rate (0.1–20*C* rate), and the rate capability increased with the increase of conducting agent (acetylene black) content as shown in Fig. 8(a). However, as the amount of conducting agent exceeded over 5 wt.%, the increase of rate capability was saturated. At the acetylene black content up to 20 wt.%, the capacity of as-received $LiMn_2O_4$ decreased about 50% at the 20*C* rate (2400 mA/g). The rate capability of $LiCoO_2$-coated $LiMn_2O_4$ improves abruptly in comparison with that of as-received $LiMn_2O_4$. For example, with the addition of 3 wt.% acetylene black, $LiCoO_2$-coated $LiMn_2O_4$ had better rate capability than as-received $LiMn_2O_4$ with the addition of 20 wt.% acetylene black. Besides, $LiCoO_2$-coated $LiMn_2O_4$ with only 7 wt.% conducting agent maintained more than 80% of its maximum capacity at a 20*C* rate

Table 1
ICP analysis of $LiCoO_2$-coated $LiMn_2O_4$ powder

| | Li | Mn | Co |
|---|---|---|---|
| Amount (mol%) | 34 | 63.8 | 2.2 |

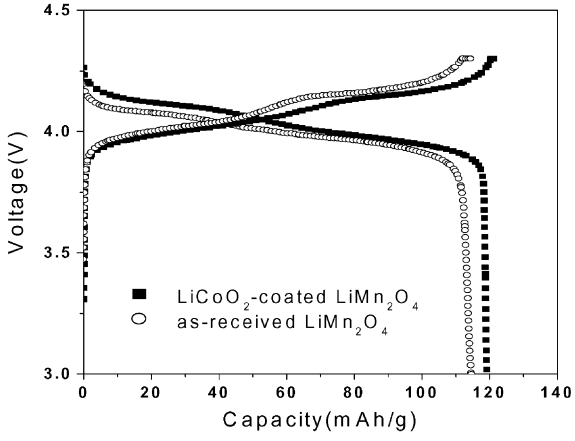


Fig. 6. Voltage vs. capacity diagram for the cells with active electrode materials of as-received $LiMn_2O_4$ and $LiCoO_2$-coated $LiMn_2O_4$ at the rate of 24 mA/g between 3.0 and 4.3 V.

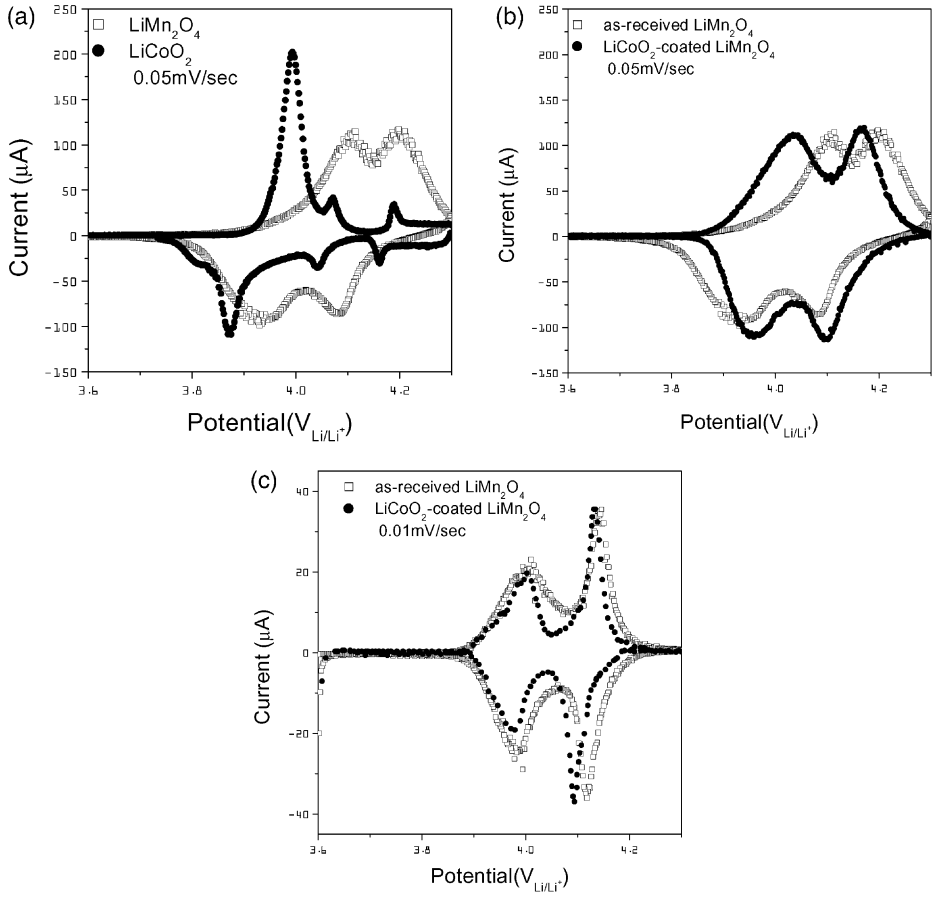


Fig. 7. Cyclic voltammetry curves of $LiCoO_2$, as-received $LiMn_2O_4$ and $LiCoO_2$-coated $LiMn_2O_4$ during charging and discharging: (a) $LiCoO_2$ and as-received $LiMn_2O_4$ at a scan rate of 0.05 mV/s, (b) as-received $LiMn_2O_4$ and $LiCoO_2$-coated $LiMn_2O_4$ at a scan rates of 0.05 mV/s and (c) 0.01 mV/s.

(2400 mA/g). To analyze these results, EIS experiments were performed on both samples. The thickness of both electrodes was 50 μm and the coated area of the electrodes was 1 $cm^2$. EIS graphs of as-received $LiMn_2O_4$ and $LiCoO_2$-coated $LiMn_2O_4$ in Fig. 9 show two semicircles, respectively. Fan and Fedkiw reported that the first semicircle in high frequency range originated from the interfacial impedance of the Li anode and might contain the contribution of the passivation film caused by the reaction between oxide and electrolyte, and the second semicircle might contain the contribution of the contact resistance between inter-particles, such as oxide–oxide, carbon–oxide, and carbon–carbon in the composite cathode [18]. Especially, the high catalytic activity of $LiMn_2O_4$ accelerates the

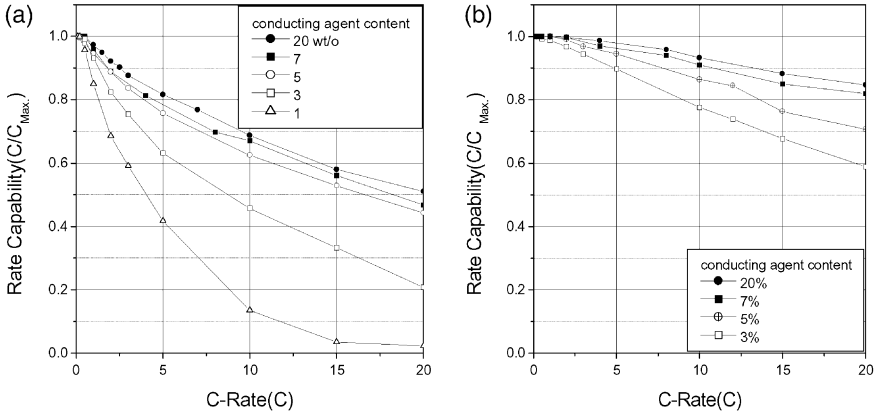


Fig. 8. Changes of normalized discharge capacity ($C/C_{Max}$) for the cells with active electrodes of (a) as-received $LiMn_2O_4$ and (b) $LiCoO_2$-coated $LiMn_2O_4$ at a varying charge–discharge rate (0.1–20$C$ rate) with the conducting agent.

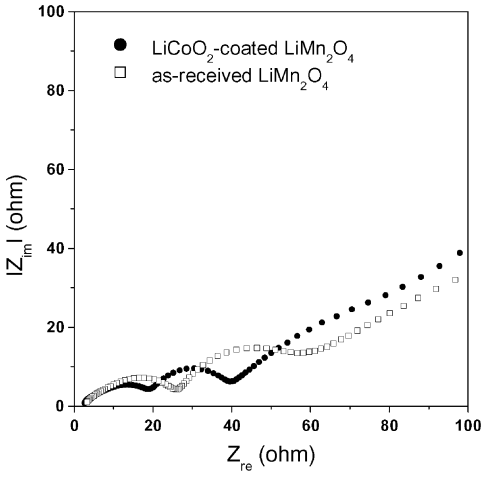


Fig. 9. EIS spectra of as-received $LiMn_2O_4$ and $LiCoO_2$-coated $LiMn_2O_4$ charged until 4.1 V.

formation of passivation film on the electrode surface due to the decomposition of electrolyte, which results in the enlargement of the first semicircle. In comparison with semicircles of as-received $LiMn_2O_4$, the first and second semicircles of $LiCoO_2$-coated $LiMn_2O_4$ were reduced. On the assumption that the interfacial impedance of Li anode of both cells is equal because both cells use the same Li anode, the shrinkage of the first semicircle in the EIS graph of $LiCoO_2$-coated $LiMn_2O_4$ means that the formation of passivation film is suppressed. The suppressed formation of passivation film can be ascribed to the lower catalytic activity of $LiCoO_2$ than that of $LiMn_2O_4$. The passivation film with organic substances acts as an electronic insulating layer and retards a current flow. Therefore, it can be proposed that the increased rate capability of $LiCoO_2$-coated $LiMn_2O_4$ is related to the improvement of current flow facilitated by the decrease of passivation film. In addition,

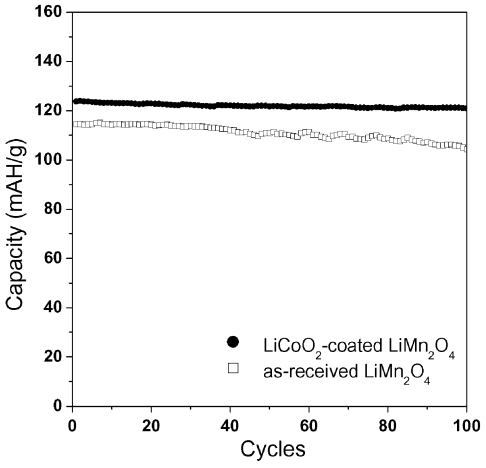


Fig. 10. Capacity vs. cycle number diagram for the cells with active electrodes of as-received $LiMn_2O_4$ and $LiCoO_2$-coated $LiMn_2O_4$ at room temperature.

the EIS analysis of $LiCoO_2$-coated $LiMn_2O_4$ shows a smaller second semicircle, which results from the decrease of inter-particle contact resistance because $LiCoO_2$ has a higher electrical conductivity ($10^{-2}$ S/cm) than $LiMn_2O_4$ ($10^{-6}$ S/cm). Consequently, the improvement of the rate capability of $LiCoO_2$-coated $LiMn_2O_4$ can be explained with the following two statements. The first reasoning is the decrease of surface film that acts as an electronic insulation layer. The second one is the inter-particle contact resistance lowered by higher electrical conductivity of $LiCoO_2$. Fig. 10 shows the cycle stabilities of as-received $LiMn_2O_4$ and $LiCoO_2$-coated $LiMn_2O_4$ at room temperature. These cells from both materials were cycled 100 times at a constant current density of 120 mA/g (1*C* rate) between 3.0 and 4.3 V. Both as-received $LiMn_2O_4$ and $LiCoO_2$-coated $LiMn_2O_4$ show an excellent cycle stability, which means that the cycle stability is also maintained after $LiCoO_2$-coating.

## 4. Conclusions

For the improvement of the rate capability, the surface of $LiMn_2O_4$ was coated with very fine $LiCoO_2$ particulates prepared by sol–gel method. The $LiCoO_2$-coated $LiMn_2O_4$ was annealed at 800°C for 6 h to crystallize $LiCoO_2$. The amount of $LiCoO_2$ content in $LiCoO_2$-coated $LiMn_2O_4$ analyzed by the ICP was about 7 mol%. $LiCoO_2$-coated $LiMn_2O_4$ showed a higher discharge capacity (120 mAh/g) than as-received $LiMn_2O_4$ (115 mAh/g) maintaining the same excellent cycle stability. Especially, the rate capability of $LiCoO_2$-coated $LiMn_2O_4$ improved significantly. The rate capability of $LiCoO_2$-coated $LiMn_2O_4$ was increased by more 60% at the 20*C* rate (2400 mA/g) in comparison with that of as-received $LiMn_2O_4$. As well, $LiCoO_2$-coated $LiMn_2O_4$ with 3 wt.% conducting agent had a higher rate capability than as-received $LiMn_2O_4$ with 20 wt.% conducting gent, which resulted in the increase of energy density in batteries. The improved rate capability is attributed to the decrease of passivation film and inter-particle contact resistance.

## Acknowledgements

The authors wish to express thanks to the Research Park of LG Chemical Ltd. for its partial financial support of this work.

## References

[1] T. Nagura, K. Tazawa, Prog. Batteries Sol. Cells 9 (1990) 20.
[2] K. Ozawa, Solid State Ionics 69 (1994) 212.
[3] G. Nagasubramanian, D. Ingersoll, D. Doughty, D. Radzykewycz, C. Hill, C. Marsh, J. Power Sources 80 (1999) 116.
[4] A.G. Ritchie, C.O. Giwa, J.C. Lee, P. Bowles, A. Gilmour, J. Allan, J. Power Sources 80 (1999) 128.

[5] M. Juzkow, J. Power Sources 80 (1999) 286.
[6] Y. Gao, M.V. Yakovleva, W.B. Ebner, Electrochem. Solid State Lett. 1 (1998) 117.
[7] J.R. Dahn, E.W. Fuller, M. Obrovac, U. von Sacken, Solid State Ionics 69 (1994) 265.
[8] M. Broussely, P. Biensan, B. Simon, Electrochim. Acta 45 (1999) 3.
[9] M.M. Thackeray, Prog. Solid State Chem. 25 (1997) 1.
[10] J.-M. Tarascon, US Patent No. 6,295-714 (1995).
[11] R. Brittihn, R. Herr, D. Hoye, J. Power Sources 43/44 (1993) 223.
[12] D. Guyomard, J.-M. Tarascon, J. Electrochem. Soc. 140 (1993) 3071.
[13] M. Yoshio, A. Ozawa, Lithium-Ion Secondary Battery, The Nikkan Kogyo Shimbun Ltd., Japan, 1996, p. 5.
[14] Y.-K. Sun, I.-H. Oh, S.-A. Hong, J. Mater. Sci. 31 (1996) 3617.
[15] Y.-K. Sun, Solid State Ionics 100 (1997) 115.
[16] H. Wang, Y.-I. Jang, B. Huang, D.R. Sadoway, Y.-M. Chiang, J. Electrochem. Soc. 146 (1999) 473.
[17] Y.-I. Jang, B. Huang, H. Wang, D.R. Sadoway, Y.-M. Chiang, J. Electrochem. Soc. 146 (1999) 3217.
[18] J. Fan, P.S. Fedkiw, J. Power Sources 72 (1998) 165.